Introduction of acetyl-phosphate bypass and increased culture temperatures enhanced growth-coupled poly-hydroxybutyrate production in the marine cyanobacterium Synechococcus sp. PCC7002

Inabe, Kosuke ; Hidese, Ryota ; Kato, Yuichi ; Matsuda, Mami ; Yoshida, Takanobu ; Matsumoto, Keiji ; Kondo, Akihiko ; Sato, Shunsuke ;…

(Citation)
Metabolic Engineering,88:228-239

(Issue Date)
2025-03

(Resource Type)
journal article

(Version)
Version of Record

Metabolic Engineering 88 (2025) 228–239

Contents lists available at ScienceDirect

Metabolic Engineering

journal homepage: www.elsevier.com/locate/meteng

Introduction of acetyl-phosphate bypass and increased culture temperatures enhanced growth-coupled poly-hydroxybutyrate production in the marine cyanobacterium *Synechococcus* sp. PCC7002

Kosuke Inabe [a,1], Ryota Hidese [a,1], Yuichi Kato [a], Mami Matsuda [a], Takanobu Yoshida [a,b], Keiji Matsumoto [c], Akihiko Kondo [a,b,d], Shunsuke Sato [c], Tomohisa Hasunuma [a,b,d,*]

[a] *Engineering Biology Research Center, Kobe University, 1-1 Rokkodai, Nada, Kobe, 657-8501, Japan*
[b] *Graduate School of Science, Technology, and Innovation, Kobe University, 1-1 Rokkodai, Nada, Kobe, Hyogo, 657-8501, Japan*
[c] *Green Planet Research Group, Agri-Bio & Supplement Research Laboratories, KANEKA CORPORATION, 1-8 Miyamae-Cho, Takasago-Cho, Takasago-city, Hyogo, 676-8688, Japan*
[d] *Research Center for Sustainable Resource Science, RIKEN, 1-7-22 Suehiro, Tsurumi, Yokohama, Kanagawa, 230-0045, Japan*

ARTICLE INFO

Keywords:
Photosynthesis
Cyanobacteria
PHA
Phosphoketolase
Metabolomics
Acetyl-phosphate bypass

ABSTRACT

Polyhydroxyalkanoate (PHA) is an attractive bio-degradable plastic alternative to petrochemical plastics. Photosynthetic cyanobacteria accumulate biomass by fixing atmospheric CO_2, making them promising hosts for sustainable PHA production. Conventional PHA production in cyanobacteria requires prolonged cultivation under nutrient limitation to accumulate cellular PHA. In this study, we developed a system for growth-coupled production of the PHA poly-hydroxybutyrate (PHB), using the marine cyanobacterium *Synechococcus* sp. PCC 7002. A recombinant strain termed KB1 expressing a set of heterologous PHB biosynthesis genes (*phaA/phaB* from *Cupriavidus necator* H16 and *phaE/phaC* from *Synechocystis* sp. PCC 6803) accumulated substantial PHB during growth (11.4% of dry cell weight). To improve PHB accumulation, we introduced the *Pseudomonas aeruginosa* phosphoketolase gene (*pk*) into strain KB1, rewiring intermediates of the Calvin–Benson–Bassham (CBB) cycle (xyluose-5-phosphate, sedoheptulose 7-phosphate, and fructose-6-phosphate) to acetyl-CoA. The *pk*-expressing strain, KB15, accumulated 2.1-fold enhanced levels of PHB (23.8% of dried cell weight), relative to the parent strain, KB1. The highest PHB titer of KB15 strain supplemented with acetate was about 1.1 g L^{-1} and the yield was further enhanced by 2.6-fold following growth at 38 °C (0.21 g L^{-1} d^{-1}), relative to growth at 30 °C. Metabolome analysis revealed that pool sizes of CBB intermediates decreased, while levels of acetyl-CoA increased in strain KB15 compared with strain KB1, and this increase was further enhanced following growth at 38 °C. Our data demonstrate that acetyl-phosphate generated by Pk was converted into acetyl-CoA via acetate by hitherto unidentified enzymes. In conclusion, expression of heterologous PHB biosynthesis genes enabled growth-coupled PHB production in strain PCC 7002, which was increased through acetyl-CoA supplementation by bypassing acetyl-phosphate and elevating culture temperature.

1. Introduction

Land and ocean pollution by petrochemical plastic wastes is an urgent concern across the globe. Bio-degradable plastics that can be degraded by natural microorganisms are attracting worldwide attention as alternatives to petrochemical plastics. Polyhydroxyalkanoate (PHA) is one such promising bio-degradable plastic that can be synthesized by several microorganisms. PHA has favorable physical properties compared with other bio-degradable plastics such as polylactic acids and is synthesized by enzymatic reactions in the host (Chen and Patel, 2012). PHA synthases catalyze polymerization of monomers such as (*R*)-3-hydroxybutyrate, (*R*)-3-hydroxy hexanoate, 4-hydroxybutyrate, and 3-hydroxyvalerate into the polymeric plastic (Tanaka et al., 2021; Verlinden et al., 2007; Zhang et al., 2015; Bhati and Mallick, 2015). To generate PHA with diverse physical properties, monomer composition can be altered by modifying the catalytic activity and expression of PHA

* Corresponding author. Engineering Biology Research Center, Kobe University, 1-1 Rokkodai, Nada, Kobe 657-8501, Japan.
E-mail address: hasunuma@port.kobe-u.ac.jp (T. Hasunuma).
[1] These authors contributed equally to this article.

https://doi.org/10.1016/j.ymben.2025.01.004
Received 29 August 2024; Received in revised form 29 December 2024; Accepted 12 January 2025
Available online 21 January 2025

synthases and other enzymes responsible for monomer synthesis (Tanaka et al., 2021; Arikawa and Matsumoto, 2016; Tan et al., 2021; Bugnicourt et al., 2014; Nduko and Taguchi, 2021).

There are two major approaches to producing value-added chemicals using microorganisms: one relies on heterotrophic microorganisms that utilize carbohydrate sources primarily derived from terrestrial plants, while the other involves autotrophic microorganisms, such as photosynthetic microorganisms, to directly produce chemicals from CO_2. Chemical production using photosynthetic organisms faces challenges, such as the low productivity of target compounds due to their slow growth rates compared to model heterotrophic microorganisms, including *Escherichia coli* and *Saccharomyces cerevisiae*. On the other hand, environmental issues of feedstock production as organic carbon sources must be considered. For instance, deforestation for plantation development results in substantial greenhouse gas emissions, while nitrogen fertilizers are a known source of the greenhouse gas nitrous oxide (Scharlemann and Laurance, 2008). Agricultural and agro-industrial residues (e.g., lignocellulosic biomass), primarily composed of cellulose, hemicellulose, and lignin, are highly promising renewable carbon sources; however, the current process for converting these feedstocks into simple sugars, such as glucose, remains challenging (Sanderson, 2011; Tarasov et al., 2018).

Cyanobacteria, which are photosynthetic microorganisms capable of CO_2 fixation, represent a sustainable and environmentally friendly system for the production of value-added chemicals. They can be genetically engineered to enable the direct conversion of CO_2 into various chemicals, including PHA, thereby contributing to mitigation of increasing atmospheric CO_2 concentrations (Arias et al., 2021). Compared to conventional crop plants, cyanobacteria exhibit faster growth rates and can be cultured on non-arable land. Moreover, they can utilize wastewater or saltwater (Machado and Atsumi, 2012). Based on these characteristics, the use of cyanobacteria for chemicals production has the potential to offer significant environmental advantages.

Several cyanobacteria, such as *Synechocystis* sp. PCC 6803 and *Nostoc muscorum*, can synthesize and accumulate the PHA-related compound poly-hydroxybutyrate (PHB) under nutrient starvation (Carpin et al., 2020; Miyake et al., 1996; Mallick et al., 2007). In cyanobacteria, PHB is synthesized from acetyl-coenzyme A (Ac-CoA) via three enzymatic steps involving β-keto thiolase (PhaA), acetoacetyl-CoA reductase (PhaB), and PHA synthase (PhaE and PhaC complex), respectively (Numata et al., 2015) (Fig. 1). *Synechococcus elongatus* PCC 7942 and *Synechococcus* sp. PCC 7002 (PCC 7002) do not encode PHB synthesis genes, but PHB synthesizing-strains can be generated by introducing a set of heterologous PHA synthesis genes (Takahashi et al., 1998; Akiyama et al., 2011).

PHB production and accumulation in cyanobacteria generally requires nutrient limitation. The highest titer (1597.1 mg L^{-1}) and productivity (0.064 g L^{-1} day^{-1}) of PHB production in cyanobacteria was reported in *Aulosira fertilissim* (Samantaray and Mallick, 2012) (Table 1), but this yield required 20 days for bacterial growth, and 5 days for PHB accumulation. Similarly, PHB production using *Synechocystis* sp. PCC 6714, has been reported to achieve 0.037 g L^{-1} day^{-1} PHB production, but this yield required 6 days of bacteria growth and 21 days for PHB accumulation (Kamravamanesh et al., 2018)(). One route to improve cyanobacterial PHB productivity is to couple growth to PHB synthesis (referred to as a growth-coupled strategy hereafter). Growth-coupled PHB production was previously reported in an engineered strain of *Synechococcus elongatus* UTEX 2973. PHB productivity in this study (0.042 g L^{-1} day^{-1}) was lower than that observed in *A. fertilissim*, predominantly because of the significantly lower PHB content (16.7% in *S. elongatus* UTEX 2973 and 85.1% in *A. fertilissim*) (Roh et al., 2021). Nutrient starvation (including nitrogen and phosphorus) effectively enhances PHB accumulation (Shinghon et al., 2021; Carpin et al., 2017), because cyanobacteria accumulate Ac-CoA and consequently PHB under such conditions (Monshupanee et al., 2016; Hirokawa et al., 2020). To achieve high levels of PHB productivity under nutrient-rich conditions, it is therefore crucial to increase cellular Ac-CoA levels (Zhu et al., 2022).

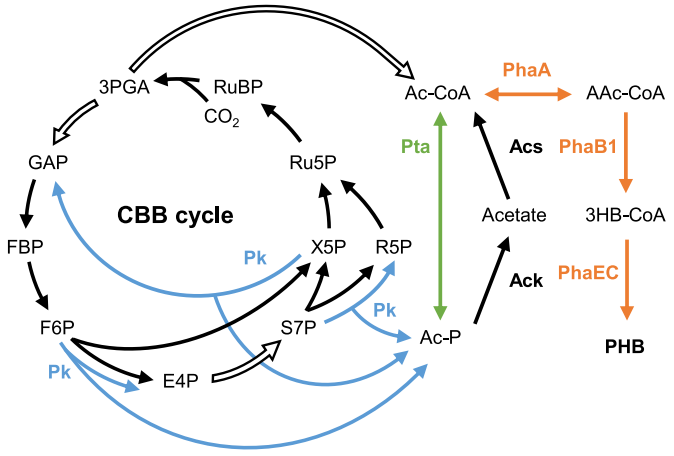

Fig. 1. The metabolic pathway of PHB biosynthesis in the recombinant *Synechoccus* sp. PCC7002 strain. Reactions by phosphoketolase (blue arrows), phosphotransacetylase (green arrow), PhaA, PhaB1, PhaEC complex (orange arrows) were developed by introducing heterologous genes. Black and white arrows represent direct and indirect reaction, respectively. Abbreviation: CBB cycle; Calvin–Benson–Bassham cycle; RuBP, ribulose 1,5-bisphosphate; GAP, glyceraldehyde 3-phosphate; FBP, fructose 1,6-bisphosphate; F6P, fructose 6-phosphate; E4P, erythrose 4-phosphate; S7P, sedoheptulose 7-phosphate; X5P, xylulose 5-phosphate; R5P, ribose 5-phosphate; Ru5P, ribulose 5-phosphate; 3PGA, 3-phosphoglycerate; Ac-CoA, acetyl-coenzyme A; AAc-CoA, acetoacetyl-coenzyme A; 3HB-CoA, 3-hydroxybutyryl-coenzyme A; Ac-P, acetyl-phosphate; PHB, poly-hydroxybutyrate; Ack, acetate kinase; Acs, acetyl-CoA synthetase; Pta, phosphotransacetylase; PhaA, β-ketothiolase; PhaB1, acetoacetyl-CoA reductase; PhaEC, PHA synthase complex; Pk, phosphoketolase. (For interpretation of the references to colour in this figure legend, the reader is referred to the Web version of this article.)

Table 1
Comparison of PHB productivity in cyanobacteria
PHB productivity (g L^{-1} day^{-1}) was calculated by dividing the PHB titer by the total cultivation time including the 1st and 2nd cultivation periods.

Organisms	Cultivation period		PHB productivity (g L^{-1} day^{-1})	Reference
	1st stage (days)	2nd stage (days)		
Aulosira fertilissima	20	5	0.064	Samantaray and Mallick (2012)
Chlorogloea fritschii TISTR 85277	16	6	0.024	Monshupanee et al. (2016)
Recombinat *Synechocystis* sp. PCC 6803	5	30	0.0068	Carpin et al., 2017
Synechocystis sp. PCC 6714	5.8	20.8	0.037	Kamravamanesh et al. (2018)
Synechococcus elongatus UTEX 2973	10		0.042	Roh et al. (2021)
Recombinat *Synechococcus* sp. PCC 7002 (KB15)	7		0.21	This study

Genetic engineering strategies to increase Ac-CoA levels have been explored previously in cyanobacteria (Samantaray and Mallick, 2012; Carpin et al., 2017; Khetkorn et al., 2016). Acetyl-phosphate (Ac-P) bypass can increase cellular Ac-CoA levels by promoting its synthesis from intermediates of the Calvin–Benson–Bassham (CBB) cycle (Zhu et al., 2022; Hirokawa et al., 2020). Phosphoketolase (Pk) is a key enzyme in this pathway which catalyzes phosphorolytic cleavage of xylulose 5-phosphate, fructose 6-phosphate, and sedoheptulose

7-phosphate (S7P) to generate Ac-P (Krüsemann et al., 2018; Liu et al., 2019) (Fig. 1). Phosphotransacetylase (Pta) subsequently mediates direct conversion of Ac-P to Ac-CoA (Miyake et al., 2000). Instead, the combination of acetate kinase (Ack) and Ac-CoA synthetase (Acs) mediates conversion of Ac-P to Ac-CoA via an acetate intermediate (Klein et al., 2007). In this context, acetate supplementation can also increase cellular Ac-CoA levels (Tarawat et al., 2020). The *pk* gene can be ectopically expressed in microorganisms harboring the *pta* or *ack/acs* genes to confer the Ac-P bypass phenotype (Kocharin et al., 2013; Chwa et al., 2016; Carpin et al., 2017). In contrast to the glycolytic pathway, Ac-P bypass generates Ac-CoA without producing CO_2 and with lower ATP consumption (Henard et al., 2015). Previous studies have demonstrated that Ac-P bypass increases the yield of Ac-CoA-derived chemicals to levels close to the theoretical maximum (Bogorad et al., 2013). Furthermore, rewiring of CBB cycle intermediates by Ac-P bypass is predicted to improve CBB cycle turnover (Xiong et al., 2015; Liu et al., 2019).

In this study, we aimed to achieve growth-coupled PHB production in cyanobacteria with improved Ac-CoA supplementation. The heterogenous PHB biosynthetic genes (*phaA/phaB1* from *Cupriavidus necator* H16 and *phaE/phaC* from *Synechocystis* sp. PCC 6803) were constitutively expressed in PCC 7002, generating the growth-coupled PHB-producing strain KB1. Ac-P bypass was conferred to KB1 by introducing the *pk* gene from *Pseudomonas aeruginosa*, which generated strain KB15 with enhanced Ac-CoA supplementation. PHB production by KB15 was enhanced by acetate supplementation and increased growth temperature. Metabolome analysis revealed that utilization of the heterogenous PHB biosynthesis pathway together with Ac-P bypass is a promising strategy to achieve high level growth-coupled PHB production.

2. Results

2.1. Development of a growth-coupled PHB-producing strain

We first aimed to generate a growth-coupled PHB-producing cyanobacterial strain. We selected strain PCC 7002 as the parent because it achieves high cell concentration with a short doubling time (3.5 h) under photoautotrophic conditions (Stevens and Porter, 1980; Frigaard et al., 2004; Ramey et al., 2015). Since strain PCC 7002 does not naturally encode PHB synthesis genes, we introduced heterologous copies of *phaA* and *phaB1* from *Cupriavidus necator* H16, and *phaE* and *phaC* from *Synechocystis* sp. PCC 6803, generating the recombinant strain KB1. To achieve PHB production under nutrient-rich conditions, these genes were expressed using strong, constitutive promoters, with *phaA* and *phaB1* expressed from the *rbcL* promoter, and *phaE* and *phaC* expressed from the *trc* promoter (Huang et al., 2010) (Fig. 2A). PHB production by KB1 was subsequently assayed under phototrophic conditions (100 μmol photons m^{-2} sec^{-1}, 1% (*v/v*) CO_2, and 30 °C). KB1 grew continuously during the cultivation period (Fig. 2B) and accumulated PHB (8.2% of dried cell weight (DCW) on day 7) (Fig. 2C). The residual cell weight (RCW), which was calculated by subtracting PHB content from total

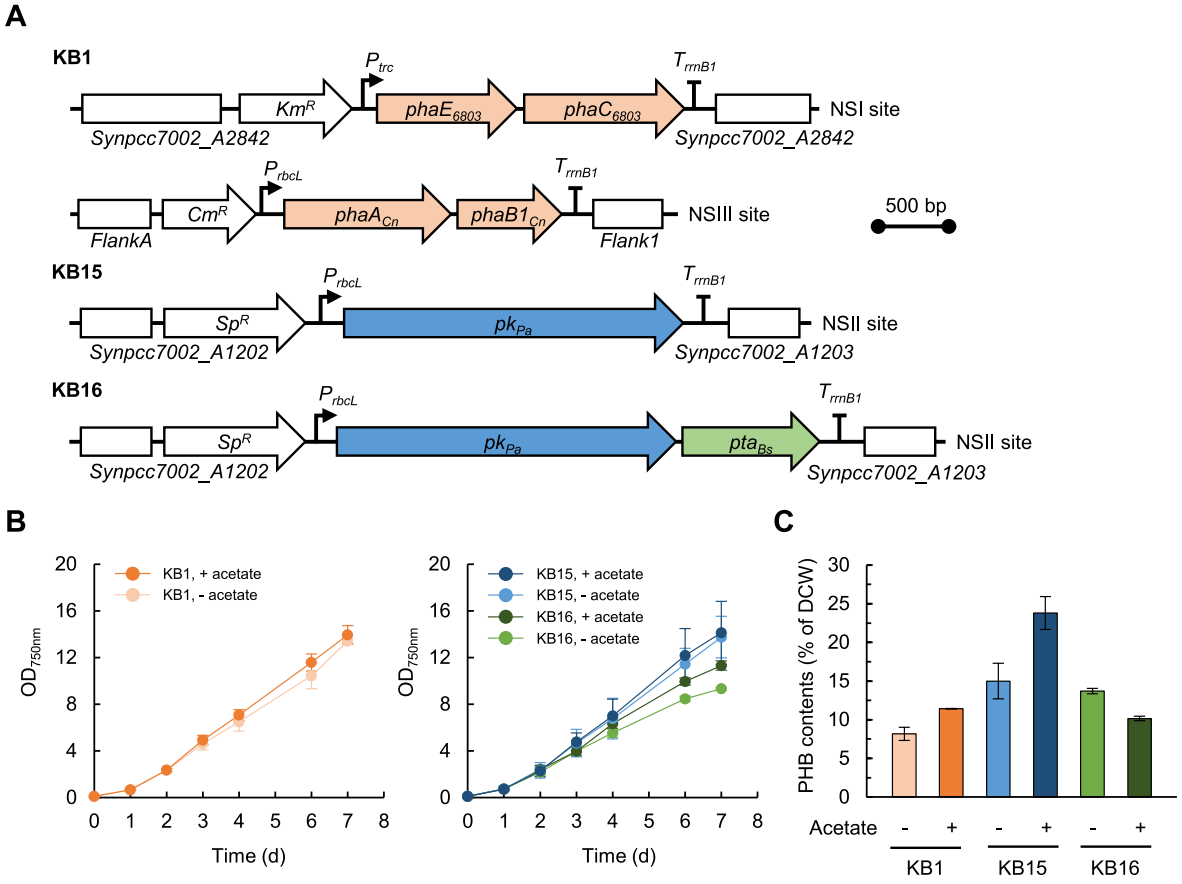

Fig. 2. Construction and evaluation of PHB-producing recombinants. (A) Genetic structures of *phaE* and *phaC* from *Synecocystis* sp. PCC6803 in the NSI site of the KB1 chromosome and *phaA* and *phaB* from *C. necator* H16 in the NSIII site of the plasmid pAQ1. Genetic structure of *pk* from *Pseudomonas aeruginosa* and tandemly arranged *P. aeruginosa pk* and *pta* from *Bacillus subtilis* in the NSII site of the KB15 and KB16 chromosomes, respectively. Abbreviations: K_m^R, kanamycin resistance gene; P_{trc}, *trc* promoter; T_{rrnB1}, *rrnB1* terminator; C_m^R, chloramphenicol resistance gene; P_{rbcL}, *rbcL* promoter; Sp^R, spectinomycin resistance gene. (B) Growth curve analysis of KB1 (left panel) and KB15 and KB16 (right panel) in the presence or absence of acetate for 7 days at 100 μmol photons m^{-2} sec^{-1}, 1% (*v/v*) CO_2, and 30 °C. (C) PHB contents of KB1, KB15, and KB16 strains grown with or without acetate at 7-day cultivation. All data are presented as means ± standard deviations (n = 3 independent biological experiments).

biomass, also continuously increased during cultivation (Supplementary Fig. S1). These results indicate that KB1 produced PHB in a growth-dependent manner. To enhance PHB accumulation in KB1, we supplemented the culture medium with 10 mM acetate. Acetate supplementation did not increase cell growth, but did lead to an 11.4% increase in PHB content in KB1 (Fig. 2C). These data suggest that increasing Ac-CoA supply is a promising approach for improving PHB accumulation in KB1.

2.2. Employing Ac-P bypass to improve Ac-CoA supply

Studies in PCC 6803 demonstrated that expression of the *Pseudomonas aeruginosa pk* gene, which encodes phosphoketolase (Pk), enhanced Ac-CoA supply, increasing the titer of the Ac-CoA derivative, 1-butanol (Liu et al., 2019). 1-butanol titers were further increased following expression of the *Bacillus subtills pta* gene, which encodes phosphotransacetylase (Pta). PCC 7002 does not naturally encode the *pk* and *pta* genes. We therefore introduced the *pk* and *pta* genes into KB1 and expressed them under control of the *rbcL* promoter to increase

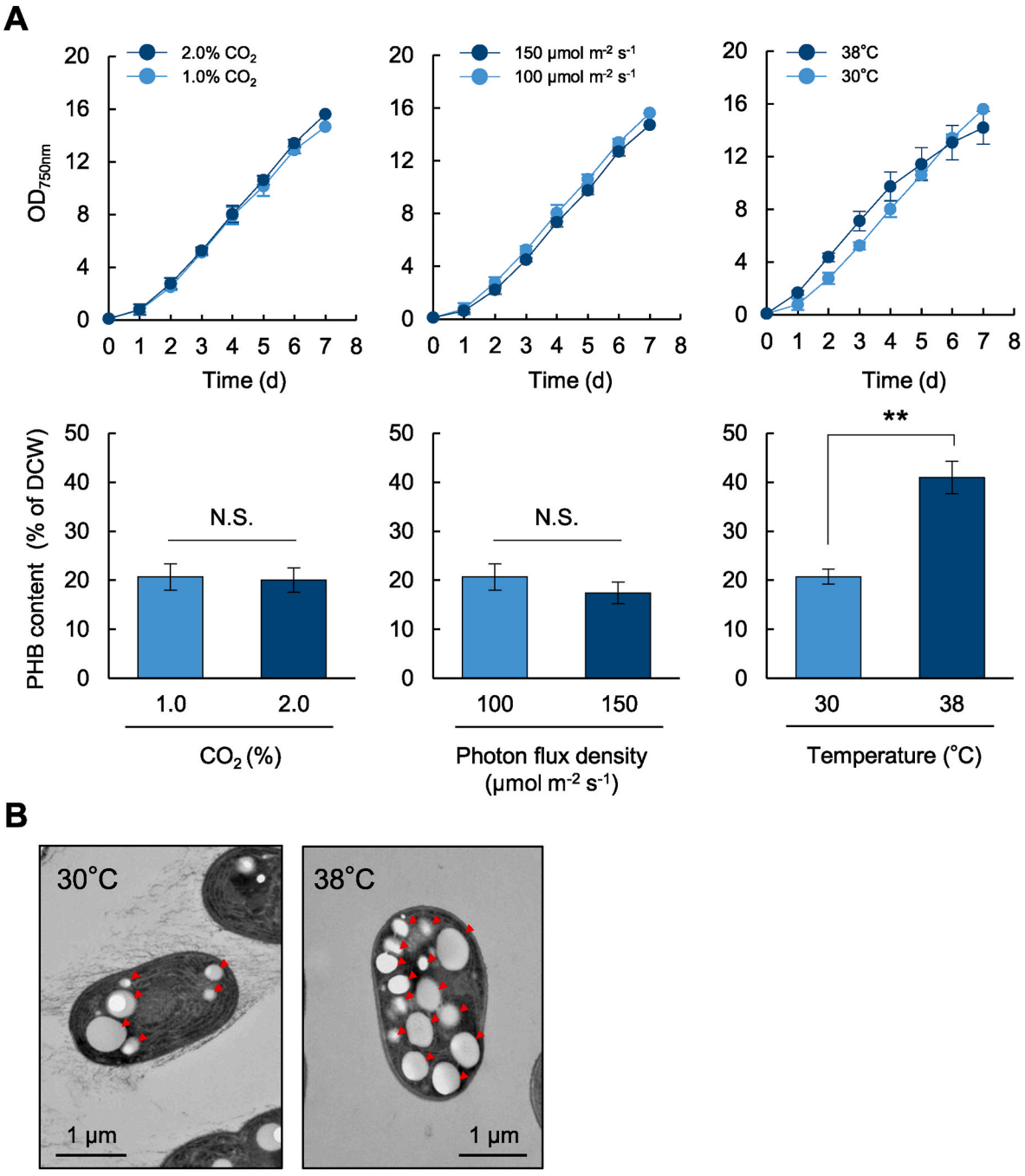

Fig. 3. Influence of cultivation conditions on PHB production in strain KB15. (A) The cell growth (OD_{750nm}) and PHB content of KB15 under different CO_2 concentrations (*v*/*v*) (left panels), light intensities (middle panels), and temperatures (right panels) were analyzed. The basic cultivation conditions were 1% (*v*/*v*) CO_2, 100 µmol photons m^{-2} sec^{-1}, and 30 °C. (B) KB15 cells were imaged by transmission electron microscopy at 30 °C and 38 °C. Red arrowheads indicate intracellular PHB granules. All data are presented as means ± standard deviations ($n = 3$ independent biological experiments). Statistical significance was determined using Welch's *t*-test (**: $P < 0.01$). N.S. ; not significant. (For interpretation of the references to colour in this figure legend, the reader is referred to the Web version of this article.)

Ac-CoA supply (Fig. 2A). The recombinant strains harboring *pk* alone and both *pk* and *pta* were denoted KB15 and KB16, respectively. Growth of KB15 was comparable to that of KB1 (Fig. 2B), but in the absence of acetate supplementation, PHB content of KB15 (14.1%) was higher than that of KB1 (8.2%) (Fig. 2C). Following acetate supplementation, the PHB content of KB15 increased to 23.8%. By contrast, growth of KB16 was lower than that of KB1 and KB15 (Fig. 2B). Indeed, without acetate supplementation, the PHB content of KB16 (13.7%) was comparable to that of KB15 (14.1%). Following addition of acetate, growth of KB16 increased, while PHB production decreased. The *pta* gene derived from *Bacillus subtilis*, introduced as a foreign gene to the KB15 strain, is physiologically known as an enzyme that catalyzes the conversion of acetyl-CoA to Ac-P (Presecan-Siedel et al., 1999). Since the PHB content of KB16 was lower than that of KB15, we consider that an excessive amount of acetyl-CoA might be conveted to acetyl-P by Pta reaction. Together, these data demonstrate that introduction of *pk* alone can increase PHB production.

2.3. High temperatures enhance PHB production in KB15

To further increase PHB production in strain KB15, we assayed different culture conditions including: CO_2 concentration, light intensity, and temperature. The standard culture conditions used in this study were 1% (*v*/*v*) CO_2, 100 μmol photons m^{-2} sec^{-1}, and 30 °C. Increasing the CO_2 concentration from 1% to 2% did not influence growth or PHB accumulation of KB15 (Fig. 3A). No significant change was observed in KB15 growth or PHB accumulation when the light intensity was increased from 100 μmol photons m^{-2} sec^{-1} to 150 μmol photons m^{-2} sec^{-1} (Fig. 3A). By contrast, the PHB content of KB15 significantly increased from 21.7% to 41.0% when cultured at 38 °C, with no significant difference in growth (Fig. 3A). We trialed combinations of each culture condition, but found that increasing growth temperature to 38 °C alone was sufficient to enhance PHB accumulation in KB15 (Supplementary Fig. S2). Transmission electron microscopy (TEM) confirmed that cells cultured at 38 °C contained more PHB granules than those grown at 30 °C (Fig. 3B).

2.4. Detailed evaluation of PHB production in KB15

Next, we measured a time course of PHB production in KB15, by determining the DCW (g L^{-1}), RCW (g L^{-1}), PHB content (% of DCW), and PHB production (g L^{-1}). During the 7 day cultivation period, DCW and RCW in the KB15 culture continuously increased regardless of acetate supplementation and/or culture temperature (Fig. 4A and B). The

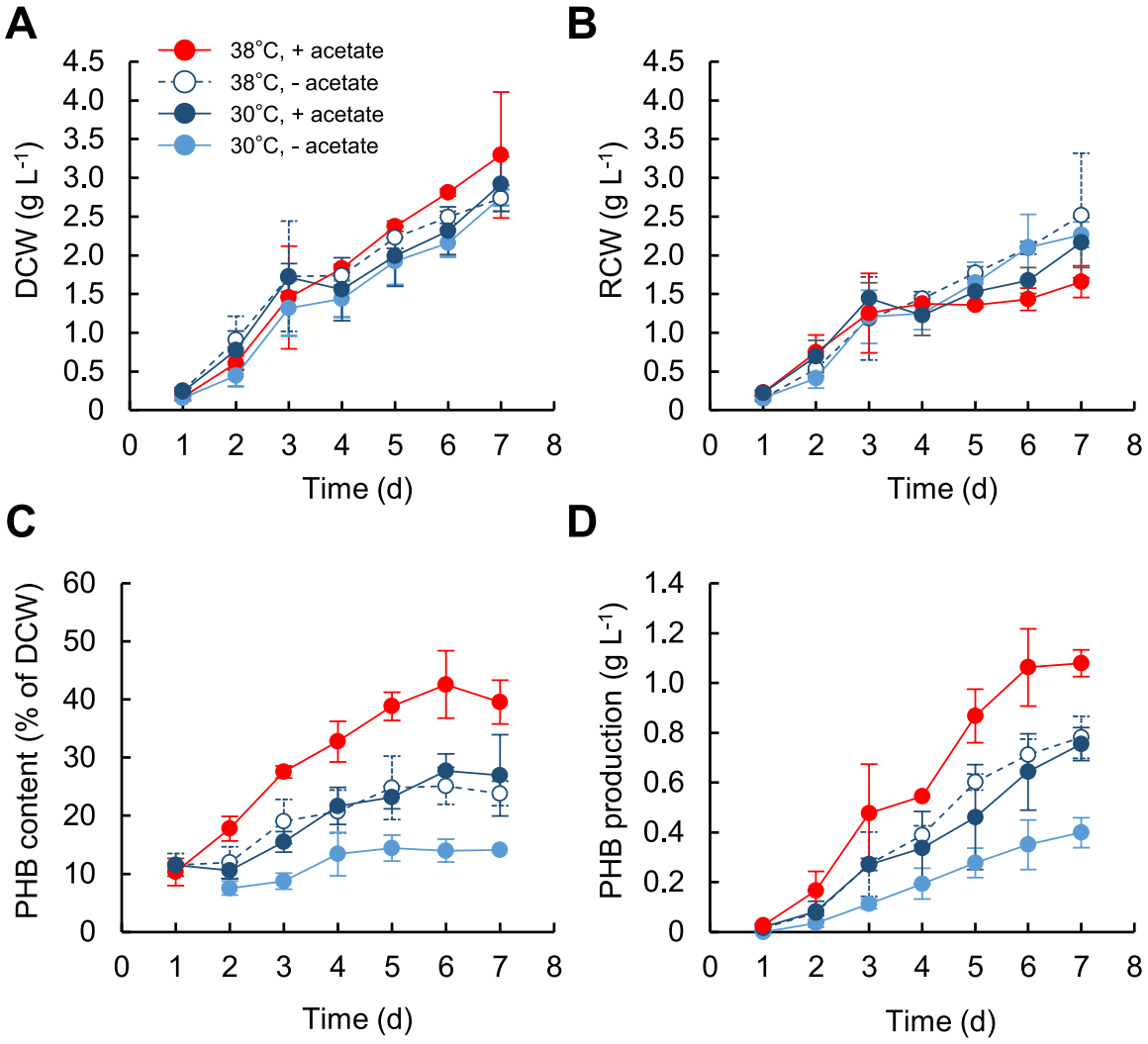

Fig. 4. Time-course analysis for PHB production **in strain KB15.** The cultivation conditions were set to 17.3 mM $NaNO_3$, 1% (*v*/*v*) CO_2, 100 μmol photons m^{-2} sec^{-1}. The cell weight, PHB content and production were compared by changing the cultivation temperatures in the presence or absence of acetate. PHB production of KB15 and its accumulation ratio was determined over time. (A) Dry cell weight (DCW) and (B) Residual cell weight (RCW) of KB15 strain. (C) PHB content and (D) PHB production of KB15 strain. All data are presented as means ± standard deviations (n = 3 independent biological experiments).

PHB content of KB15 was enhanced by both acetate supplementation and increasing culture temperature (Fig. 4C). Since PHB content increased together with RCW during cultivation, KB15 displayed growth-coupled PHB production even with acetate supplementation and higher culture temperatures. The highest PHB content was achieved with acetate supplementation at 38 °C (42.6%) (Fig. 4C). Reflecting the high PHB content, the highest PHB titer was also achieved with acetate supplementation at 38 °C (1.1 g L^{-1}) (Fig. 4D). At 30 °C, PHB productivity of KB15 was 0.076 g L^{-1} d^{-1} without the addition of acetate, and 0.15 g L^{-1} d^{-1} with acetate. At 38 °C, PHB productivity was 0.14 g L^{-1} d^{-1} without acetate and 0.21 g L^{-1} d^{-1} with acetate. Thus, strain KB15 showed the highest PHB productivity at 38 °C and in the presence of acetate.

2.5. Metabolic determinants of enhanced PHB production

To determine the metabolic basis for enhanced PHB production through Ac-P bypass, we analyzed the metabolic pool sizes in KB1 and KB15 by capillary electrophoresis time-of-flight mass spectrometry (CE-TOFMS). In the CBB cycle, KB15 showed significantly higher accumulation of fructose 1,6-bisphosphate (FBP) than KB1 (Fig. 5). The additional CBB cycle metabolites 3-phosphoglycerate (3PGA), sedoheptulose 7-phosphate (S7P), fructose 6-phosphate (F6P), ribose 5-phosphate (R5P), ribulose 5-phosphate (Ru5P), and ribulose 1,5-bisphosphate (RuBP) were present in decreased levels in KB15 relative to KB1. At 38 °C, levels of 3PGA, S7P, R5P, and Ru5P were lower in KB15 than in KB1. This disparity may be because several metabolites in the CBB cycle had been converted by Pk. The ratio of adenosine 5′-triphosphate (ATP) to the combined levels of ATP and adenosine 5′-diphosphate (ADP) (ATP/(ATP + ADP)) in KB15 were significantly smaller than in KB1 throughout the cultivation period. These data suggest that metabolite flux in the CBB cycle was enhanced by intermediate consumption through Ac-P bypass, increasing the utilization of ATP. Considering the glycolytic pathway, strain KB15 showed significantly lower levels of 3PGA, 2-phosphoglycerate (2PGA), and phosphoenolpyruvate (PEP) than KB1. By contrast, the levels of Ac-CoA were significantly higher in the KB15 than in KB1 (Fig. 5), indicating that Ac-CoA supplementation was improved by Ac-P bypass. In the tricarboxylic acid (TCA) cycle, KB15 showed smaller metabolic pool sizes than KB1. At multiple time points, the levels of citrate, isocitrate, succinate,

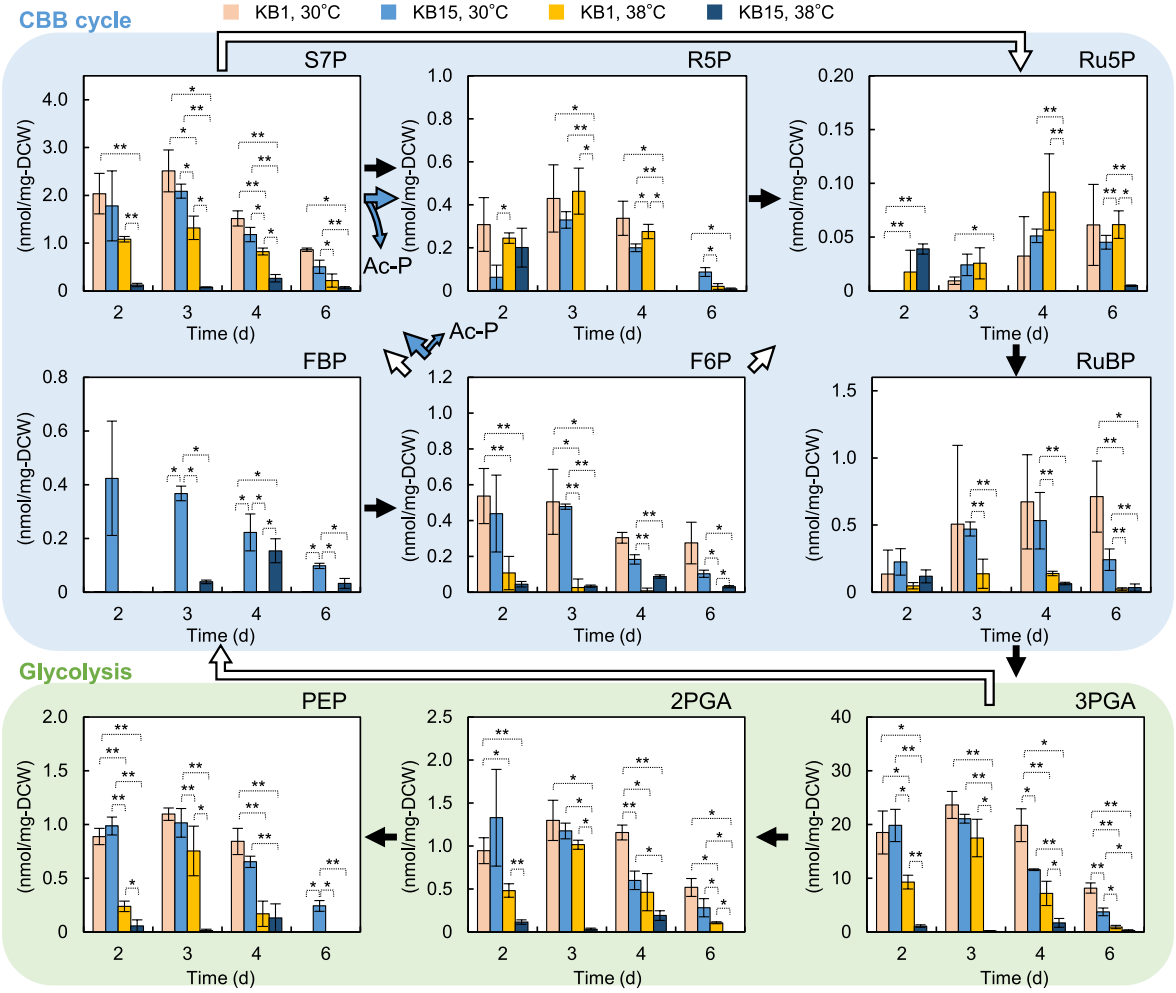

Fig. 5. Metabolome analysis of strains KB1 and KB15. Time-course changes in intracellular metabolite pool sizes of strains KB1 and KB15 at 30 °C or 38 °C at each cultivation period. Comparison of the abundance of selected metabolites in the CBB cycle, glycolytic pathway, TCA cycle, and PHB synthesis pathway are shown. Black and white arrows represent direct and indirect reaction, respectively. Blue and orange arrows indicate the reactions by phosphoketolase and PHB biosynthetic enzymes PhaABEC, respectively. Abbreviations: 2PGA, 2-phosphoglycerate; 3PGA, 3-phosphoglycerate; Ac-CoA, acetyl-CoA; 3HB-CoA, 3-hydroxybutyryl-CoA; ADP, adenosine-diphosphate; ATP, adenosine-triphosphate; F6P, fructose 6-phosphate; FBP, fructose 1,6-bisphosphate; PEP, phosphoenolpyruvate; PHB, poly-hydroxybutyrate; R5P, ribose 5-phosphate; Ru5P, ribulose 5-phosphate; RuBP, ribulose 1,5-bisphosphate; S7P, sedoheptulose 7-phosphate; TCA, tricarboxylic acid. All data are presented as means ± standard deviations ($n = 3$ independent biological experiments). Statistical significance was determined using Dunnett's test (*: $P < 0.05$, **: $P < 0.01$). Absence of a line between each bar indicates no statistical significance. (For interpretation of the references to colour in this figure legend, the reader is referred to the Web version of this article.)

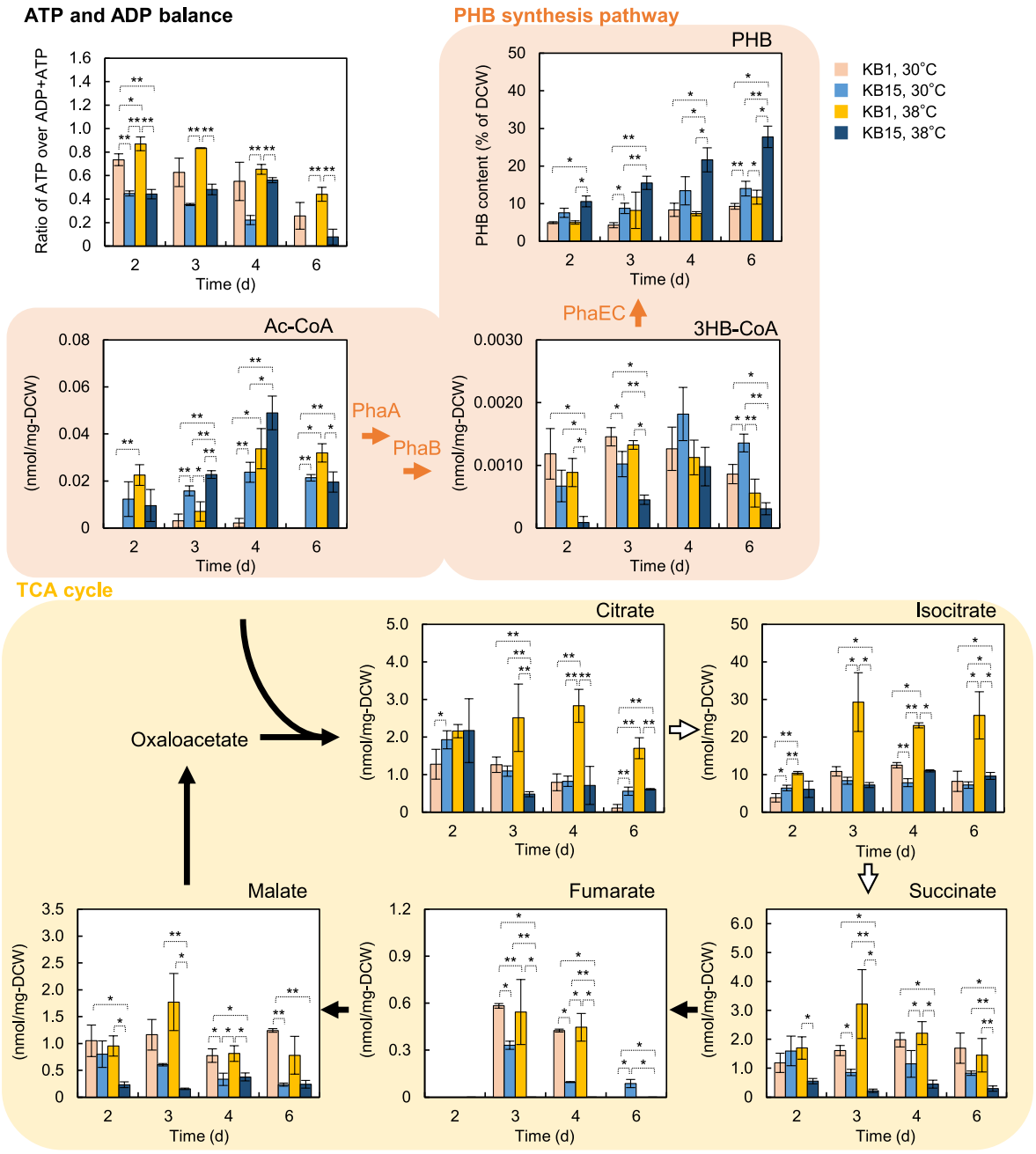

Fig. 5. (*continued*).

fumarate, and malate were significantly lower in KB15 than in KB1. These results suggest that in KB15, the metabolic flux from Ac-CoA might be partitioned into PHB synthesis, rather than toward the TCA cycle.

We also examined the metabolic basis of PHB production at enhanced temperatures using metabolome analysis. Considering the CBB cycle and glycolysis, levels of FBP, S7P, F6P, R5P, Ru5P, 3PGA, 2PGA, and PEP in strain KB15 were significantly lower at 38 °C than at 30 °C. This was also the case for most metabolites of the TCA cycle. By contrast, levels of Ac-CoA in KB15 were not significantly different at 38 °C than at 30 °C. These results suggest that temperature elevation can increase levels of Ac-CoA by enhancing metabolic flux from the CBB cycle and glycolysis and suppressing metabolic flux toward the TCA cycle. Indeed, the levels of 3-hydroxybutyryl-CoA (3HB-CoA) were lower at 38 °C than at 30 °C, suggesting that the metabolic flux downstream of the 3HB-CoA was enhanced by temperature elevation.

2.6. Characterizing the Ac-P conversion pathway

Metabolome analysis revealed that Ac-CoA supplementation was enhanced in KB15 following ectopic expression of the *pk* gene when compared with KB1. This suggested that PCC 7002 can naturally convert Ac-P into Ac-CoA. However, while neither the *pta* or *ack* genes have been identified in PCC 7002, a gene encoding Acs is annotated in the genome sequence (NCBI locus tag: SYNPCC7002_A2015). To clarify the mechanism of Ac-P conversion, we determined enzymatic activity in cell extracts from PCC 7002. Generation of Ac-CoA was monitored through the coupling of malate dehydrogenase and citrate synthetase using absorbance of NADH at 340 nm (A_{340nm}) as the readout (Castaño-Cerezo et al., 2009, 2012) (Fig. 6A). The A_{340nm} of the cell extract remained unchanged following addition of Ac-P (Fig. 6B), suggesting that PCC 7002 does not have Pta activity. A_{340nm} increased however, when the cell extract was incubated with Ac-P and ADP (Fig. 6B). ADP is required

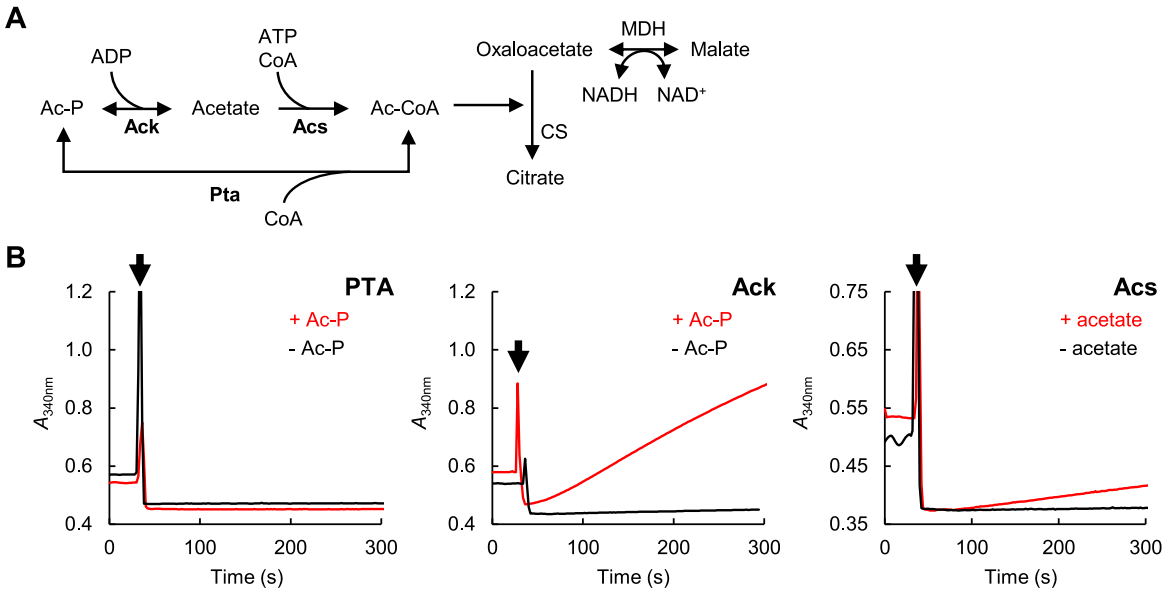

Fig. 6. Identification of the acetyl-P to acetyl-CoA conversion pathway. (A) The acetyl-CoA biosynthesis pathway from acetyl-P involves a one-step reaction by phosphotransacetylase (Pta) or a two-step reaction by acetate kinase (Ack) and acetyl-CoA synthetase (Acs). To detect the activities leading to acetyl-CoA synthesis, a coupling assay with both malate dehydrogenase (MDH) and citrate synthase (CS) was performed considering that the rate of NADH formation is limited by acetyl-CoA production rate. The assay was performed using a whole-cell lysate from PCC 7002. The principle of the assay is summarized by scheme. (B) Each reaction was carried out with (red) or without (black) the corresponding substrate with CoA for phosphotransacetylase (Pta, left panel), ADP for acetate kinase (Ack, middle panel), and CoA and ATP for acetyl-CoA synthetase (Acs, right panel). Arrow indicates the timing of the addition of the corresponding substrate. (For interpretation of the references to colour in this figure legend, the reader is referred to the Web version of this article.)

for dephosphorylation of Ac-P by acetate kinase. The A_{340nm} also increased following addition of acetate (Fig. 6B), indicating that in KB15, Ac-P generated by Pk is converted into Ac-CoA by Acs and an unidentified Ack enzyme.

2.7. Enzymatic activity in the PHB synthesis pathway

Metabolome analysis suggested that conversion of 3HB-CoA, which is catalyzed by the PhaEC complex, was enhanced by introduction of the *pk* gene and increased culture temperature (Fig. 5). To examine this hypothesis, we determined the enzymatic activity of the PhaEC complex in whole-cell lysates of KB1 and KB15 by quantifying CoA levels using Ellman's reagent (5,5′-dithio-bis-(2-nitrobenzoic acid: DTNB), which increases in absorbance at 412 nm (A_{412nm}) following reaction with the thiol group in CoA. The enzymatic activity of the PhaEC complex was higher in KB15 than in KB1 at both 30 °C and 38 °C (Fig. 7A). Furthermore, PhaEC activities in both strains did not differ when comparing incubation at 30 °C and 38 °C. These results suggest that introduction of the *pk* gene, but not increased culture temperature, enhanced conversion of 3HB-CoA into PHB. We also determined the role of Ac-P on PHA synthase activity using KB1, but observed no significant difference in this assay either in the presence or absence of Ac-P (Fig. 7B).

3. Discussion

3.1. Influence of pk expression on cyanobacterial metabolism

In this study, we achieved growth-coupled PHB production by constitutively expressing heterologous PHB synthesis genes (Fig. 4). PHB production was enhanced by introduction of the *pk* gene, which drives Ac-P bypass via acetate (Fig. 6), and by temperature elevation

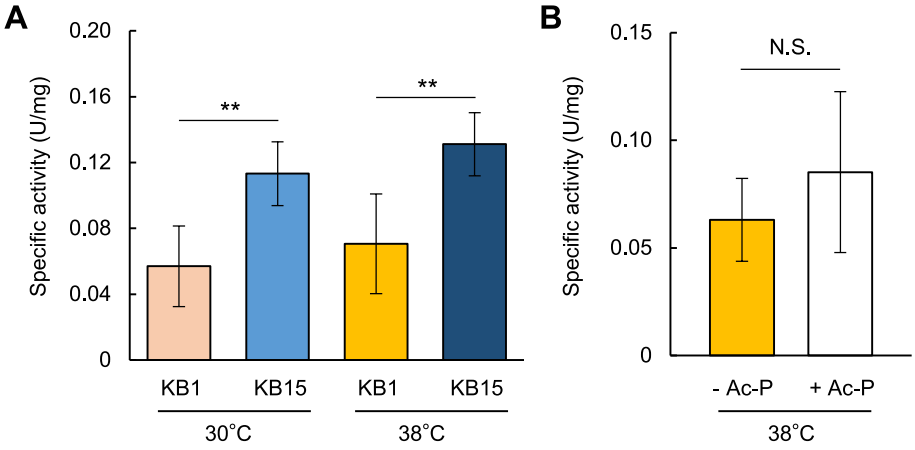

Fig. 7. Activities of the PHA synthase PhaEC of KB1 and KB15 strains. (A) The PhaEC activities in KB1 and KB15 were measured at 30 °C or 38 °C. (B) PHA synthase activity in KB1 was measured with (+Ac-P) or without (-Ac-P) Ac-P supplementation. All data are presented as means ± standard deviations ($n = 3$ independent biological experiments). Statistical significance was determined using Dunnett's test (**: $P < 0.01$). N.S. ; not significant.

(Fig. 3A). Strain KB15 showed higher Ac-CoA levels than strain KB1 (Fig. 5), suggesting that introduction of the *pk* gene alone contributed to increased Ac-CoA supplementation. Since Pk catalyzes generation of Ac-P, we hypothesized that PCC 7002 harbors enzymes for Ac-P conversion into Ac-CoA. One such enzyme is Pta, but no *pta* gene has been identified in the PCC 7002 genome (Ludwig and Bryant, 2011). Additionally, no homologous genes to the gene encoding acetate kinase from either *Synechocystis* sp. PCC 6803 (UniProt ID: P73162) or *Synechococcus elongatus* PCC 7942 (UniProt ID: Q31LG0) were identified by the NCBI BLAST program (https://www.ncbi.nlm.nih.gov). The other candidate mechanism for conversion of Ac-P into Ac-CoA is a combination of Ack and Acs. Indeed, we detected Ack and Acs enzymatic activities in whole-cell lysates of PCC 7002 (Fig. 6B), suggesting that in KB15, intermediate metabolites of the CBB cycle were rewired into Ac-CoA through Ac-P bypass via acetate.

Several reports have discussed the driving force in the acetyl-P bypass pathway: (1) *n*-butanol production in a recombinant *Synechocystis* sp. PCC 6803 (Anfelt et al., 2015) and (2) formatotrophic growth of a recombinant *Cupriavidus necator* H16 (Janasch et al., 2022). In a recombinant *Synechocystis* sp. PCC 6803, the CBB and Ac-P bypass pathway demonstrated higher theoretical butanol productivity than the CBB and Embden–Meyerhof–Parnas pathway, with reduced ATP demand for butanol synthesis (Anfelt et al., 2015). Additionally, *C. necator* can utilize formate as its sole carbon and energy source. Formate is metabolized via formate dehydrogenases, and the resulting CO_2 is assimilated through the CBB cycle. It has been shown that introduction of foreign *pk* increases the total driving force toward acetyl-CoA, as revealed by elementary flux mode analysis (Janasch et al., 2022). In the present study, Ac-P bypass caused significant reductions of 3PGA, S7P, R5P, and Ru5P in the CBB cycle of the KB15 (Fig. 5). Levels of ATP were significantly lower in KB15 than in KB1, suggesting that acetyl-P bypass would contribute to the turnover of the CBB cycle, while ensuring that the reducing power NADPH is directed toward PHB production. KB15 showed accumulation of FBP, which could also be caused by enhanced turnover of the CBB cycle because bifunctional fructose-1, 6-bisphosphatase/sedoheptulose-1,7-bisphosphatase is a bottleneck enzyme in this process (De Porcellinis et al., 2018).

3.2. Temperature elevation decreases pool sizes of metabolites in the central metabolic pathway for high PHB production

Increased culture temperatures improved PHB accumulation in KB15 from 21% (30 °C) to 41% (38 °C) (Fig. 3A) and the PHB productivity from 0.15 g L^{-1} d^{-1} (30 °C) to 0.21 g L^{-1} d^{-1} (38 °C). These observations likely correlate with reduced levels of several metabolites in the CBB cycle and the glycolytic pathway at this temperature (Fig. 5). Temperature generally affects the catalytic activity of enzymes (Daniel and Danson, 2013) as evidenced in previous reports showing that a temperature shift from 30 °C to 40 °C enhanced glycolytic flux in *Escherichia coli* (Wittmann et al., 2007). Together, this indicates that increased temperature also enhances enzymatic activities within the glycolytic pathway and CBB cycle in PCC 7002. By contrast, conversion of 3HB-CoA into PHB was remained unchanged by the increase in temperature (Fig. 7). We therefore suggest that increased temperature improved PHB production by enhancing metabolic flux in the glycolytic pathway and CBB cycle. Furthermore, conversion of 3HB-CoA is not the bottleneck to PHB production in KB15, and was not enhanced by increased temperatures.

3.3. PHA synthase activation drives higher PHB production

PHB production in KB15 was higher than that of KB1, while no significant increase in 3HB-CoA levels were observed during cultivation. Similarly, increased temperature improved PHB accumulation and productivity in KB15, but did not alter 3HB-CoA levels. High PHB production levels do not therefore necessarily correlate with 3HB-CoA accumulation. To examine the consumption of 3HB-CoA, we measured PHA synthase activity, and found higher levels of enzymatic activity in KB15 compared with KB1 (Fig. 7A). Given our enzymatic assay data (Fig. 7B), we suggest that PHA synthase activity is not affected by the addition of Ac-P. Another possible reason for high PHB production in KB15 is that the stability of PhaC is increased by Ac-P through non-enzymatic acetylation. Post-translational modifications have been reported to stabilize enzymes by preventing their degradation (Lee et al., 2023). Indeed Ac-P is involved in post-translational modifications such as acetylation and phosphorylation to regulate gene expression and enzyme activity, and acetylation of proteins by Ac-P can occur non-enzymatically (Christensen et al., 2019). Previous studies have also demonstrated that PHA synthase activity in cyanobacteria is enhanced by addition of Ac-P to the cell lysis solution (Miyake et al., 1997; Sharma et al., 2006), and that the PhaC protein is acetylated in PCC 6803 (Mo et al., 2015). These reports are consistent with the hypothesis that Ac-P stabilizes the PhaC protein via non-enzymatical acetylation.

3.4. Utility of a growth-coupled strategy for PHB production

Conventionally, cultivation under nutrient-limited conditions has been used for PHB production in cyanobacteria (Carpin et al., 2017; Shinghon et al., 2021). This culture method produces high PHB titers, but is laborious as it requires a first stage of cultivation under nutrient-replete conditions for cell growth, before a second stage of cultivation under nutrient-limited conditions for PHB accumulation. In previous studies, the highest PHB productivity (0.064 g L^{-1} d^{-1}) was achieved in *Aulosira fertilissima* after a total of 25 days cultivation (Samantaray and Mallick, 2012) (Table 1). In this study, we achieved PHB productivity levels of 0.20 g L^{-1} d^{-1} in a growth-coupled system, which is 3.1-fold higher than in *Aulosira fertilissima*, after only 7 days of cultivation. Thus, the growth-coupled PHB production strategy established in this study can produce PHB following shorter cultivation periods, which is consequently useful to achieve high PHB productivity. Since PHB accumulates intracellularly in microorganisms, the increase in the cell density and growth rate of KB15 strain is essential for improving PHB titer and productivity. Acetate supplementation has been shown to increase PHB titer in PHB-producing recombinant cells (Fig. 2). Therefore, an overexpression and/or catalytic activity enhancement of Acs could effectively enhance PHB titer in photo-mixotrophic production.

A significant drawback of cyanobacteria-based production is their slower growth rate. A photobioreactor would enable high-cell-density cultivation of the KB15 strain through controlled high light intensity and CO_2 supply. Higher light intensities may induce oxidative stress in cyanobacteria, leading to growth inhibition through photodamage and photoinhibition (Hamilton, 2019). Therefore, improving the photosynthetic efficiency and CO_2 fixation capacity of cyanobacteria is critical for enhancing growth rates and achieving higher final cell densities. Our preliminary results demonstrated that the growth rate and final cell density of KB15 cells increased under a higher light intensity (500 μmol photon m^{-2} s^{-1}) compared to cultivation at 100–150 μmol photon m^{-2} s^{-1}; however, glycogen accumulation was observed instead of PHB in the KB15 strain under the conditions, suggesting that photosynthetically fixed carbon was preferentially allocated to glycogen. Future study is necessary to develop strains that optimize carbon flux towards PHB production under high-cell-density cultivation conditions.

4. Materials and methods

4.1. Strains and culture conditions

The cyanobacterium *Synechococcus* sp. PCC 7002 and the recombinant strains were cultivated in double-deck flasks using A2 medium containing 17.3 mM $NaNO_3$ (Hasunuma et al., 2014, 2019) in the presence of 1% CO_2 (*v/v*). Cells were inoculated at an optical density of

750 nm (OD_{750nm}) of 0.1 and were cultured under continuous illumination with white, fluorescent lamps at 100 μmol photons m^{-2} s^{-1} at 30 °C or 38 °C with rotary shaking at 100 rpm.

4.2. Construction of recombinant strains

To construct the vector for integration at the NSI site (Begemann et al., 2013) (between 2,967,447 bp and 2,965,814 (−) bp), the 5′-flanking and 3′-flanking regions of *Synpcc7002_A2842* were separately amplified with a set of primers A2842-Fw1/A2842-Rv1 and A2842-Fw2/A2842-Rv2 by PCR using *Synechococcus* sp. PCC7002 genomic DNA as the template. A kanamycin resistance gene cassette including the *trc* promoter and *rbcL* terminator was PCR-amplified from pSKtrc-slr0168 (Hasunuma et al., 2016) by using primers Kan-Fw/Kan-Rv. The DNA fragments of the 5′- and 3′-flanking regions of *Synpcc7002_A2842* and the kanamycin resistant gene cassette were integrated into *Kpn*I/*Hin*dIII sites of the pBluescript II SK (+) vector by In-Fusion HDR cloning kit (Takara Bio, Kusatsu, Japan), generating plasmid pSKtrc-glpKins.

To construct the vector for integration at the NSII site (Ruffing et al., 2016) (between 1,247,489 bp and 1,247,586 bp, which was at the position between *Synpcc7002_A1202* and *Synpcc7002_A1203* on the chromosome), the 5′-flanking regions of *Synpcc7002_A1202* and *Synpcc7002_A1203* genes were separately amplified with primers A1202_A1203-Fw1/A1202_A1203-Rv1 and A1202_A1203-Fw2/A1202_A1203-Rv2 by PCR using *Synechococcus* sp. PCC7002 genomic DNA as the template. A spectinomycin resistance gene and the *rbcL* promoter/terminator were separately PCR-amplified from synthesized DNA (Thermo Fisher Scientific, Waltham, MA) and pSKrbcL-Flank1-FlankB (Hasunuma et al., 2019) using primer pairs Spec-Fw/Spec-Rv and rbcL_cassete-Fw/rbcL_cassete-Rv, respectively. The DNA fragments of 5′-flanking regions of the *Synpcc7002_A1202* and *Synpcc7002_A1203* genes, the spectinomycin resistant gene cassette and the *rbcL* promoter/terminator cassette were integrated into *Eco*RI/*Hin*dIII sites of the pUC118 vector using an In-Fusion HDR cloning kit, generating in plasmid pSp-A1202.

To construct the vector for integration at the NSIII site (between 3631 bp and 4195 bp, which was at the position of 5′-upstream region of *Flank A* on the plasmid pAQ1), the *FlankA* site (512 bp) was amplified with primers FlankA-Fw/FlankA-Rv by PCR using *Synechococcus* sp. PCC7002 genomic DNA as a template. The *FlankA* site DNA fragments were integrated into *Mlu*I/*Hin*dIII sites of the pSKrbcL-Flank1-FlankB vector (Hasunuma et al., 2019) by In-fusion cloning, generating plasmid pSKrbcL-Flank1-FlankA. A chloramphenicol resistance gene was PCR-amplified from pTCP2031V (Horiuchi et al., 2010) using primers Cm-Fw/Cm-Rv. The DNA fragment of the chloramphenicol resistance gene cassette was integrated into *Xho*I/*Not*I sites of the pSKrbcL-Flank1-FlankA vector by In-fusion cloning, generating in pSCrbcL-Flank1-FlankA.

The *Synechocystis* sp. PCC6803 *phaE* (Uniprot Entry: P73389) and *phaC* (Uniprot Entry: P73390), and *Cupriavidus necator phaA* (Uniprot Entry: P14611), and *phaB1* (Uniprot Entry: A0A481XSF4) genes were separately amplified with primers phaE-Fw/phaC-Rv, phaA-Fw/phaA-Rv, and phaB1-Fw/phaB1-Rv by PCR using *Synechocystis* sp. PCC6803 and *Cupriavidus necator* H16 genomic DNA as a template. The *Pseudomonus aeruginosa pk* (Uniprot ID: Q9HY13) was amplified by PCR with a set of primers: pk-Fw1/pk-Rv1 for *pk* cloning, using the synthesized DNA (Thermo Fisher Scientific). The *P. aeruginosa pk* and *Bacillus subtilis pta* gene (Uniprot ID: P39646) were amplified by PCR with a set of primers: pk-Fw1/pk-Rv2, and pta-Fw/pta-Rv, using the synthesized DNA (Thermo Fisher Scientific). The *phaEC*, *phaA* and *phaB*, *pk,* and *pta* DNA fragments were integrated into *Eco*RI/*Xba*I sites, *Eco*RI/*Kpn*I sites, and *Eco*RI/*Kpn*I sites of the pSKtrc-glpKins, pSCrbcL-Flank1-FlankA, and pSp-A1202, by In-fusion cloning, generating plasmids pSKtrc-glpKins-phaEphaC, pSCrbcL-phaAB, pSp-A1202-PK, and pSp-A1202-PK_PTA, respectively.

Specific gene integration in *Synechococcus* sp. PCC7002 has been described previously (Hasunuma et al., 2019). Each recombinant strain was obtained by sequential 'pop-in/pop-out' gene replacement from the parent strain. The recombinant strain KB1 was obtained by transforming PCC 7002 using pSKtrc-glpKins-phaEphaC and pSCrbcL-phaAB, and the recombinant strains KB15 and KB16 were obtained by transforming the KB1 with pSp-A1202-PK and pSp-A1202-PK_PTA, respectively. The recombinant strains were selected following growth on 40 μg mL^{-1} kanamycin, 10 μg mL^{-1} chloramphenicol, and 40 μg mL^{-1} spectinomycin where appropriate. Complete segregation was confirmed by PCR using primer pairs A2842-Fw1/A2842-Rv2 for tandemly arranged *phaE* and *phaC* integration into NSI, FlankA-Fw/Flank1-Seq for tandemly arranged *phaA* and *phaB1* integration into NSIII, and A1202_A1203-Fw1/A1202_A1203-Rv2 for *pk* or tandemly arranged *pk* and *pta* integrations into NSII. The primers used in this study are listed in Supplementary Table S1.

4.3. Quantification of PHB

PHB content in cells was measured as previously described with some modifications (Zhang et al., 2015). Briefly, dried cells were mixed with 2 mL methanolysis solution containing 50% (*v/v*) chloroform, 42.5% (*v/v*) methanol, and 7.5% (*v/v*) H_2SO_4, using 2 mg L^{-1} methyl benzoate as an internal standard. Methanolysis of PHB was performed by incubating the mixture at 100 °C for 140 min. Following addition of 2 mL deionized water, the organic phase was separated for quantification of methyl 3-hydroxybutyrate. The sample was analyzed using a Shimadzu GC-17A gas chromatograph connected to a Shimadzu GCMS-QP500 mass spectrometer equipped with an Ultra ALLOY UA-5 15m column (15 m length × 0.25 mm i.d., film thickness of 0.25 μm; Frontier lab. ltd., Fukushima, Japan). The injection port was maintained at 230 °C. The injection volume was 1 μL and the split ratio was 1:8. Helium was used as the carrier gas, and the flow rate was held constant at 1.04 mL min^{-1}. The column temperature was held at 60 °C for 4 min, raised by 8 °C min^{-1} to 160 °C, held for 4 min, raised by 15 °C min^{-1} to 350 °C, and finally held for a further 4 min. Interface and ion source temperatures were maintained at 250 °C and 200 °C, respectively. Electron impact ionization was conducted at 70 eV, and the mass spectra were recorded by scanning the 100–500 *m/z* range. The analysis was simultaneously performed in the scan mode (from 85 to 500 *m/z*) and a selected ion monitoring (SIM) mode (*m/z* 118 for methyl 3-hydroxybutyrate, and *m/z* 136 for methyl benzoate) using the Shimadzu Fast Automated Scan/SIM (FASTT) mode.

4.4. Electron microscopy

Cells were collected at day 7 by centrifugation at 8000×*g* at 4 °C for 10 min. After removing the supernatant, cells were rapidly frozen in liquid propane and were subject to chemical fixation with acetone containing 2% (*v/v*) glutaraldehyde, 1% (*w/v*) tannic acid, and 2% (*v/v*) distilled water at −80 °C for 2 days. The samples were then incubated at −20 °C for 3 h, before incubation at 4 °C for 4 h. The samples were stained with 2% (*w/v*) uranyl acetate at room temperature. Ultrastructures of *Synechococcus* cells were observed by TEM (JEM-1400Plus, JEOL, Tokyo, Japan) using a Tokai Electron Microscope, Inc. (Aichi, Japan).

4.5. Metabolome analysis

Samples for metabolome analysis were prepared as previously described with minor modifications (Hasunuma et al., 2019). Briefly, a 5 mg-DCW aliquot of *Synechococcus* cells were collected at each sampling time by filtration using 1-μm pore size polytetrafluoroethylene (PTFE) disks (Merck Millipore, Billerica, MA). Samples were immediately washed with 20 mM $(NH_4)_2CO_3$ pre-cooled to 4 °C, and suspended in 4 mL methanol containing 37.4 μM methionine sulfone and 37.4 μM

piperazine-1,4-bis(2-ethanesulfonic acid) as the internal standards. 0.5 mL of the cell suspension was mixed with 0.2 mL of 4 °C water and 0.5 mL of 4 °C chloroform and suspended by vortexing for 30 s. The aqueous and organic layers were separated by centrifugation at 14,000×*g* for 5 min at 4 °C. The aqueous layer (500 μL) was filtered through a 3 kDa cut-off cellulose membrane (Millipore) to remove solubilized proteins. The sample was vacuum evaporated using a FreeZone 2.5 Plus freeze dryer system (Labconco, Kansas City, MO) and dissolved in 250 μL pure water. Intracellular metabolites were extracted and analyzed using CE-TOFMS (Agilent G7100; MS, Agilent G6224AA LC/MSD TOF; Agilent Technologies, Palo Alto, CA, USA) according to a previously reported method (Hasunuma et al., 2016). Intracellular 3HB-CoA levels were analyzed using a LCMS-8050 triple quadrupole mass spectrometer (Shimadzu Corporation, Kyoto, Japan) equipped with Atlantis T3® analytical column (150 × 2.1 mm, 3 μm particle size, 100 Å pore size). The mobile phase consisted of 50 mM ammonium acetate (pH = 6.9) as the eluent A, and acetonitrile as the eluent B. The fraction of eluent B linearly increased as reported previously (Neubauer et al., 2015). The column temperature was set to 30 °C, and other conditions were the same as in previous studies (Takenaka et al., 2021).

4.6. Ac-P conversion assay

Conversion of Ac-P into Ac-CoA was assayed as previously described (Castaño-Cerezo et al., 2012). Cells were cultivated at 38 °C and collected at day 2 by centrifugation at 8000×*g* at 4 °C for 10 min, washed once with assay buffer (25 mM Tris-HCl (pH = 7.5) containing 5% glycerol), and stored at −80 °C. For analysis, cells were resuspended with 1 mL of the assay buffer, and disrupted using 0.1 mm glass beads YGB05 and a multi-bead shocker MB1001C(S) (Yasui Kikai, Osaka, Japan) at 4 °C. After centrifugation at 10,000×*g* for 10 min at 4 °C, the supernatant was collected as a whole-cell lysate. Protein concentrations of the whole-cell lysate was determined using a Pierce BCA Protein Assay Kit (Thermofisher Scientific). An assay solution (1 mL) containing whole-cell lysate (0.375 mg of protein), 1 mM CoA, 3 mM NAD^+, 2.5 mM malate, 2.5 unit mL^{-1} malate dehydrogenase, and 1.25 unit mL^{-1} citrate synthase were prepared in assay buffer. To measure Pta activity, Ac-P was added to the assay solution at a final concentration of 10 mM. To measure Ack activity, Ac-P, $MgCl_2$, and ADP were added to the assay solution at final concentrations of 10 mM, 0.25 mM, and 0.1 mM, respectively. To measure Acs activity, acetate, $MgCl_2$, and ATP were added to the assay solution at final concentrations of 10 mM, 0.25 mM, and 0.1 mM, respectively. The assay solution was incubated at 30 °C until the absorbance at 340 nm stabilized, before addition of 100 μL of 100 mM Ac-P or acetate to initiate the enzymatic reaction. The activities were monitored by using UV–Vis spectrophotometer (JASCO Corporation, Tokyo, Japan).

4.7. Measurement of PhaEC activity

Cells were cultivated at 30 °C or 38 °C and collected at day 2 by centrifugation. Whole-cell lysates were prepared as described above using assay buffer (25 mM Tris-HCl (pH = 7.5) containing 5% glycerol). An assay solution containing whole-cell lysate (0.375 mg of protein) and 0.5 mM DTNB were prepared in the assay buffer. The solution (800 μL) was subsequently incubated at 30 °C and 38 °C for 10 min, and the PHB synthesis reaction was initiated by addition of 100 μL of 16 mM DL-3-hydroxybutyryl-CoA. PhaEC activity was monitored at an increase of absorbance at 412 nm by using UV–Vis spectrophotometer (JASCO Corporation). One unit of enzyme activity was defined for the reaction as the amount of enzyme that produced 1 μmol of 2-Nitro-5-mercaptobenzoic acid (TNB) per minute.

CRediT authorship contribution statement

Kosuke Inabe: Writing – original draft, Visualization, Validation, Methodology, Investigation, Formal analysis, Conceptualization. **Ryota Hidese:** Writing – review & editing, Writing – original draft, Methodology, Conceptualization. **Yuichi Kato:** Writing – review & editing, Methodology. **Mami Matsuda:** Methodology, Investigation, Formal analysis. **Takanobu Yoshida:** Methodology, Investigation, Formal analysis. **Keiji Matsumoto:** Writing – review & editing, Validation, Methodology, Investigation, Formal analysis, Conceptualization. **Akihiko Kondo:** Supervision, Resources. **Shunsuke Sato:** Writing – review & editing, Supervision, Project administration, Funding acquisition, Conceptualization. **Tomohisa Hasunuma:** Writing – review & editing, Supervision, Resources, Project administration, Funding acquisition, Conceptualization.

Declaration of competing interest

The authors declare no competing financial interests.

Acknowledgments

We thank Ms. Rie Matsuyama for their technical assistance. This work was supported by the Advanced Low Carbon Technology Research and Development Program (ALCA) of the Japan Science and Technology Agency (JPMJAL1608). It was also supported by the Program for Forming Japan's Peak Research Universities (J-PEAKS) from the Japan Society for the Promotion of Science (JSPS).

Appendix A. Supplementary data

Supplementary data to this article can be found online at https://doi.org/10.1016/j.ymben.2025.01.004.

Data availability

Data will be made available on request.

References

Akiyama, H., Okuhata, H., Onizuka, T., Kanai, S., Hirano, M., Tanaka, S., Sasaki, K., Miyasaka, H., 2011. Antibiotics-free stable polyhydroxyalkanoate (PHA) production from carbon dioxide by recombinant cyanobacteria. Bioresour. Technol. 102, 11039–11042.

Anfelt, J., Kaczmarzyk, D., Shabestary, K., Renberg, B., Rockberg, J., Nielsen, J., Uhlén, M., Hudson, E.P., 2015. Genetic and nutrient modulation of acetyl-CoA levels in Synechocystis for *n*-butanol production. Microb. Cell Fact. 14, 167.

Arias, D.M., Ortíz-Sánchez, E., Okoye, P.U., Rodríguez-Rangel, H., Balbuena Ortega, A., Longoria, A., Domínguez-Espíndola, R., Sebastian, P.J., 2021. A review on cyanobacteria cultivation for carbohydrate-based biofuels: cultivation aspects, polysaccharides accumulation strategies, and biofuels production scenarios. Sci. Total Environ. 794, 148636.

Arikawa, H., Matsumoto, K., 2016. Evaluation of gene expression cassettes and production of poly(3-hydroxybutyrate-co-3-hydroxyhexanoate) with a fine modulated monomer composition by using it in *Cupriavidus necator*. Microb. Cell Fact. 15, 184.

Begemann, M.B., Zess, E.K., Walters, E.M., Schmitt, E.F., Markley, A.L., Pfleger, B.F., 2013. An organic acid based counter selection system for cyanobacteria. PLoS One 8, e76594.

Bhati, R., Mallick, N., 2015. Poly(3-hydroxybutyrate-co-3-hydroxyvalerate) copolymer production by the diazotrophic cyanobacterium *Nostoc muscorum* Agardh: process optimization and polymer characterization. Algal Res. 7, 78–85.

Bogorad, I.W., Lin, T., Liao, J.C., 2013. Synthetic non-oxidative glycolysis enables complete carbon conservation. Nature 502, 693–697.

Bugnicourt, E., Cinelli, P., Lazzeri, A., Alvarez, V., 2014. Polyhydroxyalkanoate (PHA): review of synthesis, characteristics, processing and potential applications in packaging. eXPRESS Polymer Lett 8, 791–818. https://doi.org/10.3144/expresspolymlett.2014.82.

Carpin, R., Du, W., Olivieri, G., Pollio, A., Hellingwerf, K.J., Marzocchella, A., Branco dos Santos, F., 2017. Genetic engineering of *Synechocystis* sp. PCC6803 for poly-β-hydroxybutyrate overproduction. Algal Res. 25, 117–127.

Carpin, R., Olivieri, G., Hellingwerf, K.J., Pollio, A., Marzocchella, A., 2020. Industrial production of poly-β-hydroxybutyrate from CO_2: can cyanobacteria Meet this challenge? Processes 8, 323.

Castaño-Cerezo, S., Bernal, V., Cánovas, M., 2012. Acetyl-coenzyme A synthetase (acs) assay. Bio-Protocol 2 (17). https://doi.org/10.21769/bioprotoc.256.

Castaño-Cerezo, S., Pastor, J.M., Renilla, S., Bernal, V., Iborra, J.L., Cánovas, M., 2009. An insight into the role of phosphotransacetylase (*pta*) and the acetate/acetyl-CoA node in *Escherichia coli*. Microb. Cell Fact. 8, 54.
Chen, G.Q., Patel, M.K., 2012. Plastics derived from biological sources: present and Future: a technical and environmental review. Chem. Rev. 112, 2082–2099.
Christensen, D.G., Xie, X., Basisty, N., Byrnes, J., McSweeney, S., Schilling, B., Wolfe, A. J., 2019. Post-translational protein acetylation: an Elegant mechanism for bacteria to Dynamically regulate metabolic Functions. Front. Microbiol. 10, 1604.
Chwa, J.W., Kim, W.J., Sim, S.J., Um, Y., Woo, H.M., 2016. Engineering of a modular and synthetic phosphoketolase pathway for photosynthetic production of acetone from CO_2 in *Synechococcus elongatus* PCC 7942 under light and aerobic condition. Plant Biotech. J. 14, 1768–1776.
Daniel, R.M., Danson, M.J., 2013. Temperature and the catalytic activity of enzymes: a fresh understanding. FEBS Lett. 587, 2738–2743.
De Porcellinis, A.J., Nørgaard, H., Furelos Brey, L.M., Erstad, S.M., Jones, P.R., Heazlewood, J.L., Sakuragi, Y., 2018. Overexpression of bifunctional fructose-1,6-bisphosphatase/sedoheptulose-1,7-bisphosphatase leads to enhanced photosynthesis and global reprogramming of carbon metabolism in *Synechococcus* sp. PCC 7002. Metab. Eng. 47, 170–183.
Frigaard, N.U., Sakuragi, Y., Bryant, D.A., 2004. Gene inactivation in the cyanobacterium *Synechococcus* sp. PCC 7002 and the green sulfur bacterium *Chlorobium tepidum* using *in vitro*-made DNA constructs and natural transformation. Methods Mol. Biol. 274, 325–340.
Hamilton, T. L. The trouble with oxygen: the ecophysiology of extant phototrophs and implications for the evolution of oxygenic photosynthesis. 2019. Free Radic. Biol. Med., 140, 233–249.
Hasunuma, T., Matsuda, M., Senga, Y., Aikawa, S., Toyoshima, M., Shimakawa, G., Miyake, C., Kondo, A., 2014. Overexpression of *flv3* improves photosynthesis in the cyanobacterium *Synechocystis* sp. PCC6803 by enhancement of alternative electron flow. Biotechnol. Biofuels 7, 493.
Hasunuma, T., Matsuda, M., Kondo, A., 2016. Improved sugar-free succinate production by *Synechocystis* sp. PCC 6803 following identification of the limiting steps in glycogen catabolism. Metab. Eng. Commun. 3, 130–141.
Hasunuma, T., Takaki, A., Matsuda, M., Kato, Y., Vavricka, C.J., Kondo, A., 2019. Single-stage Astaxanthin production enhances the Nonmevalonate pathway and photosynthetic central metabolism in *Synechococcus* sp. PCC 7002. ACS Synth. Biol. 8, 2701–2709.
Henard, C.A., Freed, E.F., Guarnieri, M.T., 2015. Phosphoketolase overexpression increases biomass and lipid yield from methane in an obligate methanotrophic biocatalyst. Curr. Opin. Biotechnol. 36, 83–88.
Hirokawa, Y., Kubo, T., Soma, Y., Saruta, F., Hanai, T., 2020. Enhancement of acetyl-CoA flux for photosynthetic chemical production by pyruvate dehydrogenase complex overexpression in *Synechococcus elongatus* PCC 7942. Metab. Eng. 57, 23–30.
Horiuchi, M., Nakamura, K., Kojima, K., Nishiyama, Y., Hatakeyama, W., Hisabori, T., Hihara, Y., 2010. The PedR transcriptional regulator interacts with thioredoxin to connect photosynthesis with gene expression in cyanobacteria. Biochem. J. 431, 135–140.
Huang, H.H., Camsund, D., Lindblad, P., Heidorn, T., 2010. Design and characterization of molecular tools for a Synthetic Biology approach towards developing cyanobacterial biotechnology. Nucleic Acids Res. 38, 2577–2593.
Janasch, M., Crang, N., Asplund-Samuelsson, J., Sporre, E., Bruch, M., Gynnå, A., Jahn, M., Hudson, E.P., 2022. Thermodynamic limitations of PHB production from formate and fructose in *Cupriavidus necator*. Metab. Eng. 73, 256–269.
Kamravamanesh, D., Slouka, C., Limbeck, A., Lackner, M., Herwig, C., 2018. Increased poly-β-hydroxybutyrate production from carbon dioxide in Randomly Mutated cells of cyanobacterial strain *Synechocystis* sp. PCC 6714: Mutant generation and characterization. Bioresour. Technol. 266, 34–44.
Khetkorn, W., Incharoensakdi, A., Lindblad, P., Jantaro, S., 2016. Enhancement of poly-3-hydroxybutyrate production in *Synechocystis* sp. PCC 6803 by overexpression of its native biosynthetic genes. Bioresour. Technol. 214, 761–768.
Klein, A.H., Shulla, A., Reimann, S.A., Keating, D.H., Wolfe, A.J., 2007. The intracellular concentration of acetyl phosphate in *Escherichia coli* is sufficient for direct phosphorylation of two-component response regulators. J. Bacteriol. 189, 5574–5581.
Kocharin, K., Siewers, V., Nielsen, J., 2013. Improved polyhydroxybutyrate production by *Saccharomyces cerevisiae* through the use of the phosphoketolase pathway. Biotechnol. Bioeng. 110, 2216–2224.
Krüsemann, J.L., Lindner, S.N., Dempfle, M., Widmer, J., Arrivault, S., Debacker, M., He, H., Kubis, A., Chayot, R., Anissimova, M., Marlière, P., Cotton, C.A.R., Bar-Even, A., 2018. Artificial pathway emergence in central metabolism from three recursive phosphoketolase reactions. FEBS J. 285, 4367–4377.
Lee, J.M., Hammarén, H.M., Savitski, M.M., Baek, S.H., 2023. Control of protein stability by post-translational modifications. Nat. Commun. 14, 201.
Liu, X., Miao, R., Lindberg, P., Lindblad, P., 2019. Modular engineering for efficient photosynthetic biosynthesis of 1-butanol from CO_2 in cyanobacteria. Energy Environ. Sci. 12, 2765–2777.
Ludwig, M., Bryant, D.A., 2011. Transcription profiling of the model cyanobacterium *Synechococcus* sp. strain PCC 7002 by next-Gen (SOLiD™) sequencing of cDNA. Front. Microbiol. 2, 41.
Machado, I.M., Atsumi, S., 2012. Cyanobacterial biofuel production. J. Biotechnol. 162, 50–56.
Mallick, N., Sharma, L., Singh, A.K., 2007. Poly-beta-hydroxybutyrate accumulation in *Nostoc muscorum*: effects of metabolic inhibitors. J. Plant Physiol. 164, 312–317.
Miyake, M., Kataoka, K., Shirai, M., Asada, Y., 1997. Control of poly-beta-hydroxybutyrate synthase mediated by acetyl phosphate in cyanobacteria. J. Bacteriol. 179, 5009–5013.
Miyake, M., Miyamoto, C., Schnackenberg, J., Kurane, R., Asada, Y., 2000. Phosphotransacetylase as a key factor in biological production of polyhydroxybutyrate. Appl. Biochem. Biotechnol. 84–86, 1039–1044.
Miyake, M., Erata, M., Asada, Y., 1996. A thermophilic cyanobacterium, *Synechococcus* sp. MA19, capable of accumulating poly-β-hydroxybutyrate. J. Ferment. Bioeng. 82, 512–514. https://doi.org/10.1016/s0922-338x(97)86995-4.
Mo, R., Yang, M., Chen, Z., Cheng, Z., Yi, X., Li, C., He, C., Xiong, Q., Chen, H., Wang, Q., Ge, F., 2015. Acetylome analysis reveals the involvement of lysine acetylation in photosynthesis and carbon metabolism in the model cyanobacterium *Synechocystis* sp. PCC 6803. J. Proteome Res. 14, 1275–1286.
Monshupanee, T., Nimdach, P., Incharoensakdi, A., 2016. Two-stage (photoautotrophy and heterotrophy) cultivation enables efficient production of bioplastic poly-3-hydroxybutyrate in auto-sedimenting cyanobacterium. Sci. Rep. 6, 37121.
Nduko, J.M., Taguchi, S., 2021. Microbial production of biodegradable lactate-based polymers and oligomeric building blocks from renewable and waste resources. Front. Bioeng. Biotechnol. 8, 618077.
Neubauer, S., Chu, D.B., Marx, H., Sauer, M., Hann, S., Koellensperger, G., 2015. LC-MS/MS-based analysis of coenzyme A and short-chain acyl-coenzyme A thioesters. Anal. Bioanal. Chem. 407, 6681–6688.
Numata, K., Motoda, Y., Watanabe, S., Osanai, T., Kigawa, T., 2015. Co-expression of two polyhydroxyalkanoate synthase subunits from *Synechocystis* sp. PCC 6803 by cell-free synthesis and their specific activity for polymerization of 3-hydroxybutyryl-co-enzyme A. Biochemistry 54, 1401–1407.
Presecan-Siedel, E., Galinier, A., Longin, R., Deutscher, J., Danchin, A., Glaser, P., Martin-Verstraete, I., 1999. Catabolite regulation of the pta gene as part of carbon flow pathways in *Bacillus subtilis*. J. Bacteriol. 181, 6889–6897.
Ramey, C.J., Barón-Sola, Á., Aucoin, H.R., Boyle, N.R., 2015. Genome engineering in cyanobacteria: where We are and where We need to Go. ACS Synth. Biol. 4, 1186–1196.
Roh, H., Lee, J.S., Choi, H.I., Sung, Y.J., Choi, S.Y., Woo, H.M., Sim, S.J., 2021. Improved CO_2-derived polyhydroxybutyrate (PHB) production by engineering fast-growing cyanobacterium *Synechococcus elongatus* UTEX 2973 for potential utilization of flue gas. Bioresour. Technol. 327, 124789.
Ruffing, A.M., Jensen, T.J., Strickland, L.M., 2016. Genetic tools for advancement of *Synechococcus* sp. PCC 7002 as a cyanobacterial chassis. Microb. Cell Fact. 15, 190.
Sanderson, K., 2011. Lignocellulose: a chewy problem. Nature 474, S12–S14.
Scharlemann, J.P., Laurance, W.F., 2008. Environmental science. How green are biofuels? Science 319, 43–44.
Samantaray, S., Mallick, N., 2012. Production and characterization of poly-β-hydroxybutyrate (PHB) polymer from *Aulosira fertilissima*. J. Appl. Phycol. 24, 803–814.
Sharma, L., Panda, B., Singh, A.K., Mallick, N., 2006. Studies on poly-beta-hydroxybutyrate synthase activity of *Nostoc muscorum*. J. Gen. Appl. Microbiol. 52, 209–214. https://doi.org/10.2323/jgam.52.209.
Shinghon, P., Phoraksa, O., Incharoensakdi, A., Monshupanee, T., 2021. Increased bioproduction of glycogen, lipids, and poly(3-hydroxybutyrate) under partial supply of nitrogen and phosphorus by photoautotrophic cyanobacterium *Synechocystis* sp. PCC 6803. J. Appl. Phycol. 33, 2833–2843. https://doi.org/10.1007/s10811-021-02494-0.
Stevens, S.E., Porter, R.D., 1980. Transformation in *Agmenellum Quadruplicatum*. Proc Natl Acad Sci U S A. 77, 6052–6056.
Takahashi, H., Miyake, M., Tokiwa, Y., Asada, Y., 1998. Improved accumulation of poly-3- hydroxybutyrate by a recombinant cyanobacterium. Biotechnol. Lett. 20, 183–186.
Takenaka, M., Yoshida, T., Hori, Y., Bamba, T., Mochizuki, M., Vavricka, C.J., Hattori, T., Yoshihiro Hayakawa, Y., Hasunuma, T., Kondo, A., 2021. An ion-pair free LC-MS/MS method for quantitative metabolite profiling of microbial bioproduction systems. Talanta 222, 121625.
Tan, D., Wang, Y., Tong, Y., Chen, G.Q., 2021. Grand challenges for industrializing polyhydroxyalkanoates (PHAs). Trends Biotechnol. 39, 953–963.
Tanaka, K., Yoshida, K., Orita, I., Fukui, T., 2021. Biosynthesis of poly(3-hydroxybutyrate-co-3-hydroxyhexanoate) from CO_2 by a recombinant *Cupriavidus necator*. Bioengineering (Basel) 213, 395.
Tarasov, D., Leitch, M., Fatehi, P., 2018. Lignin-carbohydrate complexes: properties, applications, analyses, and methods of extraction: a review. Biotechnol. Biofuels 11, 269.
Tarawat, S., Incharoensakdi, A., Monshupanee, T., 2020. Cyanobacterial production of poly(3-hydroxybutyrate-co-3-hydroxyvalerate) from carbon dioxide or a single organic substrate: improved polymer elongation with an extremely high 3-hydroxyvalerate mole proportion. J. Appl. Phycol. 32, 1095–1102.
Verlinden, R.A., Hill, D.J., Kenward, M.A., Williams, C.D., Radecka, I., 2007. Bacterial synthesis of biodegradable polyhydroxyalkanoates. J. Appl. Microbiol. 102, 1437–1449.
Wittmann, C., Weber, J., Betiku, E., Krömer, J., Böhm, D., Rinas, U., 2007. Response of fluxome and metabolome to temperature-induced recombinant protein synthesis in *Escherichia coli*. J. Biotechnol. 132 (4), 375–384.
Xiong, W., Lee, T.C., Rommelfanger, S., Gjersing, E., Cano, M., Maness, P.C., Ghirardi, M., Yu, J., 2015. Phosphoketolase pathway contributes to carbon metabolism in cyanobacteria. Nat. Plants 2, 15187.
Zhang, S., Liu, Y., Bryant, D.A., 2015. Metabolic engineering of *Synechococcus* sp. PCC 7002 to produce poly-3-hydroxybutyrate and poly-3-hydroxybutyrate-co-4-hydroxybutyrate. Metab. Eng. 32, 174–183.
Zhu, L., Zhang, J., Yang, J., Jiang, Y., Yang, S., 2022. Strategies for optimizing acetyl-CoA formation from glucose in bacteria. Trends Biotechnol. 40 (2), 149–165.